RAA 2019 Vol. **19** No. **7**, 99(12pp) doi: 10.1088/1674–4527/19/7/99

http://www.raa-journal.org *http://iopscience.iop.org/raa*

Research in Astronomy and Astrophysics

Photometric investigation and orbital period analyses of the W UMa binaries FP Lyn, FV CVn and V354 UMa

Raul Michel[1], Qi-Qi Xia[2] and Jesus Higuera[1]

[1] Observatorio Astronómico Nacional, Instituto de Astronomía, Universidad Nacional Autónoma de México, Apartado Postal 877, Ensenada, B.C. 22830, México

[2] Shandong Provincial Key Laboratory of Optical Astronomy and Solar-Terrestrial Environment, Institute of Space Sciences, Shandong University, Weihai 264209, China; *xiaqi77@126.com*

Received 2018 November 6; accepted 2019 February 4

Abstract New light curves and photometric solutions of FP Lyn, FV CVn and V354 UMa are presented. We found that these three systems are W-subtype shallow contact binaries. In addition, it is obvious that the light curves of FP Lyn and V354 UMa are asymmetric. Therefore, a hot spot was added on the primary star of FP Lyn and a dark spot was added on the secondary star of V354 UMa. At the same time, we added a third light to the photometric solution of FP Lyn for the final result. The obtained mass ratios and fill-out factors are $q = 1.153$ and $f = 13.4\%$ for FP Lyn, $q = 1.075$ and $f = 4.6\%$ for FV CVn, and $q = 3.623$ and $f = 10.7\%$ for V354 UMa respectively. The investigations of orbital period for these three systems indicate that the periods are variable. FP Lyn and V354 UMa were discovered to have secularly increasing components with rates of $dp/dt = 4.19 \times 10^{-7}\,\mathrm{d\,yr^{-1}}$ and $dp/dt = 7.70 \times 10^{-7}\,\mathrm{d\,yr^{-1}}$ respectively, which are feasibly caused by conservative mass transfer from the less massive component to the more massive component. In addition, some variable components were discovered for FV CVn, including a rate of $dp/dt = -1.13 \times 10^{-6}\,\mathrm{d\,yr^{-1}}$ accompanied by a cyclic oscillation with amplitude and period of 0.0069 d and 10.65 yr respectively. The most likely explanation for the long-term decrease is angular momentum loss. The existence of an additional star is the most plausible explanation for the periodic variation.

Key words: stars: binaries: close — stars: binaries: eclipsing — stars: individual (FP Lyn, FV CVn and V354 UMa)

1 INTRODUCTION

W UMa type stars are eclipsing binaries with orbital periods of usually less than one day. W UMa stars are close binaries of spectral types F, G or K. Both stars are filling or over-filling their Roche lobes, thus sharing a common convective envelope (CCE) (Lucy 1968a,b). W UMa type stars transfer energy between the two components through their CCE, and their strong interaction affects their evolution properties such as mass transfer (e.g., Li et al. 2015c, 2018; Liao et al. 2017), magnetic activity (e.g., Applegate 1992; Yuan & Qian 2007; Li et al. 2014), thermal relaxation oscillation (TRO) (e.g., Lucy 1976; Flannery 1976; Robertson & Eggleton 1977) and angular momentum loss (AML) (e.g., vant Veer 1979; Rahunen 1981; van Hamme 1982; Qian 2001a,b, 2003). Understanding these properties is also very important for studying other types of eclipsing binaries. The results of orbital period analyses have shown that the presence of a third body is a common feature of W UMa systems. Examples include V781 Tau (Li et al. 2016a), V502 Oph (Zhou et al. 2016b), TYC 1337–1137–1 and TYC 3836–0854–1 (Liao et al. 2017) and V0474 Cam (Guo et al. 2018). The observations and statistical analyses of W UMa type stars are of great significance for understanding the evolution process of eclipsing binaries (e.g., Qian et al. 2017, 2018).

FP Lyn was detected as an EW type binary star by Maciejewski & Niedzielski (2005) who found an orbital period of 0.359097 d and a maximum V magnitude of 11.36. Later, Hoffman et al. (2009) identified 4659 variable objects in the Northern Sky Variability Survey and classified FP Lyn as a W UMa candidate with an orbital period of 0.35913 d. Recently, Hubscher (2016) and Juryšek et al. (2017) reported the timing of minima for many eclipsing binaries including those of FP Lyn. Nevertheless, the related study of photometric solutions and period variations has not been published yet. Therefore, in this paper, the photometric solutions and $O - C$ analyses were obtained by using the new light curves of BVR_c and all minima times that have been observed.

FV CVn was firstly identified as an eclipsing binary system whose period is 0.31539899 d from ROTSE All-Sky Surveys for Variable Stars published by Akerlof et al. (2000). Then, as a byproduct of the ROTSE-I CCD survey, FV CVn was observed with CCD equipment by Blattler & Diethelm (2004). The period was revised as 0.315367 d and demonstrated the object to be a W UMa type binary system. Times of minima for FV CVn were obtained by several authors later, such as Diethelm (2005, 2006, 2007) and Nelson (2016). However, there has been no analysis about the physical parameters or evolutionary state of FV CVn. Recently, we observed FV CVn for two nights, and the complete light curves of BVR_cI_c were obtained. So, we analyzed the orbital period and light curves with all available data.

V354 UMa is a W UMa eclipsing binary according to ROTSE-I data (Woźniak et al. 2004). The light curves were firstly obtained by Khruslov (2006), which later demonstrated that it is a W UMa type binary whose period is 0.293825 d. From Norton et al. (2007), 11.02 mag in V band was determined. Then, some minima times were obtained from Nelson (2015), Hubscher (2016) and others. It also has no photometric analyses or period investigations. Therefore, we analyzed its light curves and orbital periods using the newly observed $UBVR_cI_c$ light curves and all available minima times in this paper.

2 OBSERVATIONS

These three objects were observed by the 84 cm telescope at the National Astronomical Observatory of Mexico (OAN-SPM) to obtain the CCD observations. Each system was observed for two nights. Standard Johnson-Cousin-Bessel $UBVR_cI_c$ filters were employed to observe these three systems. Information about the observation time, filters and exposure time of FP Lyn, FV CVn and V354 UMa is listed in Table 1. One aspect in particular is the different exposure time of FP Lyn on 2016 January 31. We changed the exposure time to obtain better observations. In order to find the best reference stars in the fields, those with color similar to the variables, the fields were calibrated during very photometric conditions and using Landolt standard stars. For FP Lyn, star 2MASSJ08420426+3905326 ($U = 12.997, B = 13.097, V = 12.544, R = 12.189, I = 11.850$) was chosen as the reference star while 2MASSJ13533984+3216259 ($U = 14.580, B = 14.684, V = 14.233, R = 13.930, I = 13.638$) was used in the case of FV CVn and TYC3466–294–1 ($U = 12.373, B = 12.286, V = 11.723, R = 11.413, I = 11.105$) for V354 UMa. The light curves of these three objects are displayed in Figure 1. It is obvious that they are all W UMa type binary systems, and the best way to explain the asymmetric light curves of FP Lyn and V354 UMa is existence of the O'Connell effect.

3 PHOTOMETRIC SOLUTIONS

The 2013 version of the Wilson-Devinney (W-D) code was applied to analyze the new light curves of FP Lyn, FV CVn and V354 UMa in order to obtain their model parameters. The initial epoch and period used to convert time into phase are as follows,

$$\begin{aligned}\text{FP Lyn: Min.}I &= 2457418.6891 + 0.359085 \times E,\\ \text{FV CVn: Min.}I &= 2458229.7505 + 0.315365 \times E,\\ \text{V354 UMa: Min.}I &= 2458231.7783 + 0.293825 \times E,\end{aligned} \tag{1}$$

where the initial epochs are calculated from our observations, the periods of FP Lyn and FV CVn are from the $O - C$ Gateway[1] and the period of V354 UMa is obtained from VSX[2].

When the W-D solutions were computed, the effective temperatures of primary stars were acquired from the Guo Shou Jing Telescope (the Large Sky Area Multi-Object Fiber Spectroscopic Telescope, LAMOST) Data Release 5[3] (e.g., Luo et al. 2015). Partial spectral information on these three systems including the effective temperatures is listed in Table 2. Therefore, we averaged their multiple observations respectively. Finally, 5907, 5470 and 5841 K were determined as T_1 for these three targets. According to Lucy (1976) and Ruciński (1969), the gravity-darkening coefficients and bolometric albedo coefficients were set as $g_{1,2} = 0.32$ and $A_{1,2} = 0.5$, respectively. Bolometric limb-darkening and bandpass limb-darkening coefficients were obtained from van Hamme (1993). Considering their light curves, it is obvious that they are all W UMa type binaries. Therefore, mode 3 was chosen for all systems during the modeling. The adjustable parameters were: orbital

[1] http://var2.astro.cz/ocgate/
[2] https://www.aavso.org/vsx/
[3] http://dr5.lamost.org/

Table 1 Information on Observations of FP Lyn, FV CVn and V354 UMa

Object	Date	Filter (Exposure time in seconds)	Type
FP Lyn	2016 January 31	$B(45)$, $V(25)$, $R_c(15)$ & $B(40)$, $V(20)$, $R_c(10)$ & $B(20)$, $V(10)$, $R_c(5)$	Complete light curves
	2016 February 20	$B(32)$, $V(16)$, $R_c(8)$	Minimum light
FV CVn	2017 March 30	$B(50)$, $V(25)$, $R_c(15)$, $I_c(15)$	Minimum light
	2018 April 21	$B(30)$, $V(20)$, $R_c(15)$, $I_c(15)$	Complete light curves
V354 UMa	2017 March 31	$B(30)$, $V(12)$, $R_c(8)$, $I_c(8)$	Minimum light
	2018 April 23	$U(40)$, $B(20)$, $V(10)$, $R_c(6)$, $I_c(6)$	Complete light curves

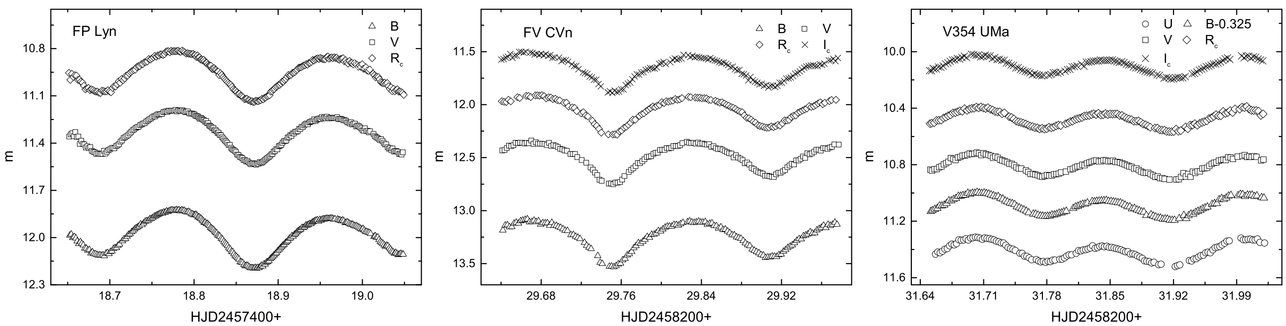

Fig. 1 CCD photometric light curves of FP Lyn (*left panel*), FV CVn (*middle panel*) and V354 UMa (*right panel*). FP Lyn: BVR_c bands observed on 2016 January 31; FV CVn: BVR_cI_c bands observed on 2018 April 21; V354 UMa: $UBVR_cI_c$ bands observed on 2018 April 23.

inclination i, effective temperature of the secondary star T_2, dimensionless potential of two components $\Omega_1 = \Omega_2$ and luminosity of primary star L_1.

As the photometric investigations of the three targets were absent since their discovery, the q-search method was implemented to determine their mass ratios. In order to find the minimum convergent solutions, we set q at fixed values from 0.1 to 10.0, and changed it in steps of 0.1. The final residuals and curves for corresponding q values are plotted in the left panels of Figures 2, 3 and 4. Then, from the three small inset figures, the q values corresponding to the minimum convergent solutions were determined as 1.4, 1.1 and 3.4, respectively. Therefore, we set them as the initial values of q and adjustable. In the meantime, other adjustable parameters were the same as before. Then the q values of convergent solutions were determined as 1.321, 1.071 and 3.299, respectively. In order to obtain better fitting results, dark spot or hot spot model and parameters of the third light were also tried during the W-D solutions.

The light curves of FP Lyn and V354 UMa are both asymmetric which indicate that the O'Connell effect exists in both of them. This is generally explained by the magnetic activity of a dark or hot spot (e.g., AD Cnc, Qian et al. 2007; GSC 03526–01995, Liao et al. 2012; V441 Lac, Li et al. 2016b; UCAC4 436–062932, Zhou et al. 2016a). Therefore, we added a hot spot or dark spot to the primary or secondary star of FP Lyn and V354 UMa, respectively. All fitting parameters are listed in Table 3. Ultimately, the fitting result with the smallest residual was selected as a hot spot on the primary star of FP Lyn and a dark spot on the secondary star of V354 UMa.

Meanwhile, we added the parameters of a third light in W-D solutions. FP Lyn and FV CVn were ultimately found to have convergent solutions, but no convergent solution was generated for V354 UMa. The parameters of the third light are also tabulated in Table 3. It is obvious that the effect of a third body on the total luminosity of FP Lyn cannot be ignored, but FV CVn has too little third light. Therefore, we just chose to add a third light to the final result for FP Lyn.

All parameters and errors were determined and are listed in Table 3. The errors were obtained by the W-D method. They are all mathematical fittings and have no meaning in terms of physics. The fitting figures of the original data and the theoretical light curves are plotted in the right panels of Figures 2, 3 and 4. All residuals (observed minus calculated, $O-C$) of these three systems are almost flat, indicating the theoretical light curves and original data were fitted well. The geometric structures at phase 0.75 for these three systems are displayed in Figure 5.

Table 2 Spectral Information on the Three Targets Acquired by LAMOST

Target	Obsdate	Subclass	[Fe/H]	$T_{\rm eff}$ (K)	$\log(g)$
FP Lyn	2014/11/20	G3	0.258	5928.24	4.182
	2014/12/08	G3	0.216	5910.85	4.202
	2014/12/26	G3	0.187	5889.37	4.138
FV CVn	2013/04/20	G7	0.006	5491.78	4.342
	2014/01/17	G7	0.064	5610.87	4.438
	2014/03/25	G7	0.057	5607.27	4.455
	2015/04/07	G7	–0.154	5253.29	4.240
	2017/02/16	G5	–0.099	5385.65	4.309
V354 UMa	2015/01/09	G0	–0.557	5811.61	4.153
	2017/03/14	G1	–0.341	5869.98	4.324
FP Lyn				5909	
FV CVn				5470	
V354 UMa				5841	

Notes: The temperatures for the primary stars of FP Lyn, FV CVn and V354 UMa that we used in calculation are 5909, 5470 and 5841 K, respectively, which are the average of their observations.

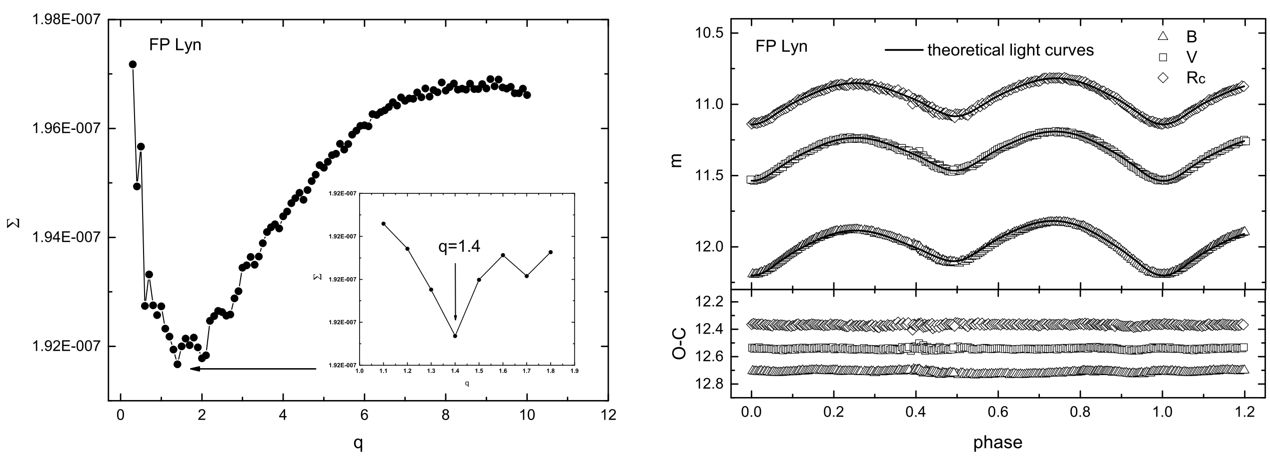

Fig. 2 The left panel is the Σ-q curves of FP Lyn. The small inset is an enlargement in which q ranges from 1.1 to 1.8. The right panel is the agreement of FP Lyn between observations and theoretical light curves derived by V, R_c and I_c light curves. It was computed with a hot spot on the primary component.

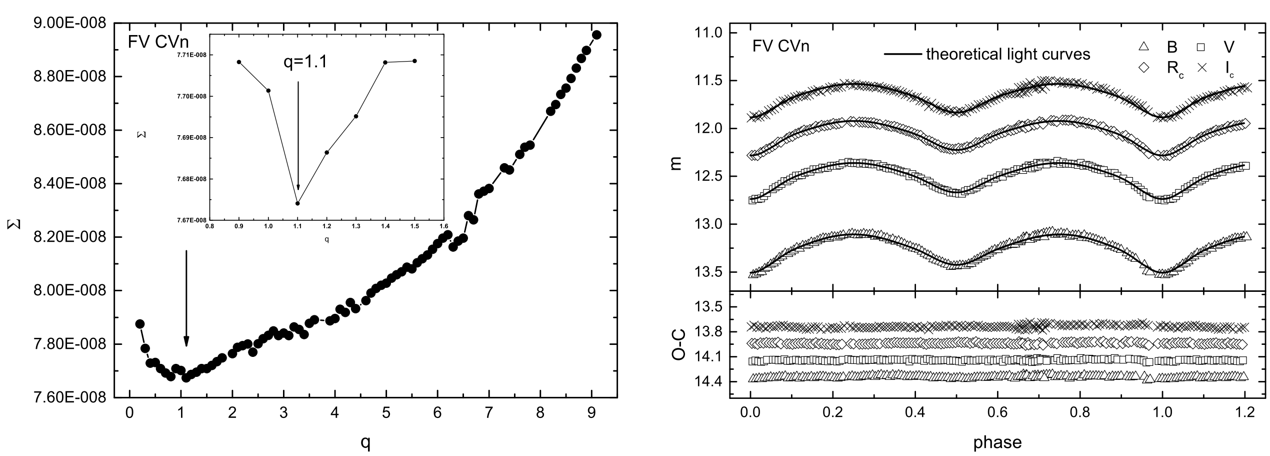

Fig. 3 The left panel is the Σ-q curves of FV CVn. The small inset is an enlargement in which q ranges from 0.9 to 1.5. The right panel is the agreement of FV CVn between observations and theoretical light curves derived by B, V, R_c and I_c light curves.

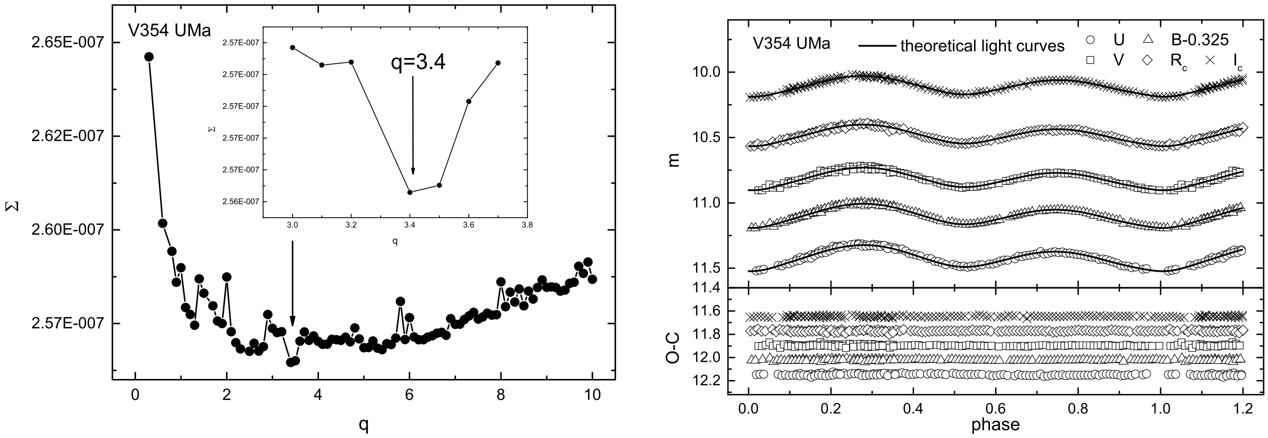

Fig. 4 The left panel is the Σ-q curves of V354 UMa. The small inset is an enlargement in which q ranges from 3.0 to 3.7. The right panel is the agreement of V354 UMa between observations and theoretical light curves derived by U, B, V, R_c and I_c light curves. It was computed with a dark spot on the secondary component.

Table 3 Photometric Solutions of FV CVn, FP Lyn and V354 UMa

Parameter	FP Lyn			FV CVn		V354 UMa	
T_1 (K)	5909	5909	5909	5470	5470	5841	5841
$q(M_2/M_1)$	1.203(7)	1.515(18)	1.153(6)	1.071(10)	1.032(25)	3.461(22)	3.622(40)
T_2 (K)	5688(15)	5255(16)	5683(14)	5120(26)	5148(24)	5745(39)	5686(33)
i (deg)	60.5(1)	59.3(1)	61.2(2)	64.2(2)	64.2(6)	50.4(7)	50.1(3)
$\Omega_{\rm in}$	4.073	4.549	4.001	3.875	3.775	7.219	7.429
$\Omega_{\rm out}$	3.513	3.970	3.445	3.325	3.230	6.594	6.802
$\Omega_1 = \Omega_2$	4.010(11)	4.465(25)	3.927(10)	3.850(13)	3.764(42)	7.174(41)	7.362(42)
L_{1U}/L_U	-	-	-	-	-	0.271(9)	0.286(8)
L_{1B}/L_B	0.517(2)	0.599(3)	0.502(4)	0.597(4)	0.608(14)	0.264(6)	0.272(5)
L_{1V}/L_V	0.502(2)	0.554(3)	0.493(3)	0.572(4)	0.580(12)	0.258(5)	0.263(4)
L_{1R_c}/L_{R_c}	0.495(2)	0.530(2)	0.481(3)	0.557(3)	0.560(12)	0.256(4)	0.259(4)
L_{1I_c}/L_{I_c}	-	-	-	0.546(3)	0.551(11)	0.254(3)	0.256(3)
L_{3U}/L_U	-	-	-	-	-	-	-
L_{3B}/L_B	-	-	0.043(2)	-	0.000(4)	-	-
L_{3V}/L_V	-	-	0.032(1)	-	0.001(3)	-	-
L_{3R_c}/L_{R_c}	-	-	0.043(1)	-	0.004(3)	-	-
L_{3I_c}/L_{I_c}	-	-	-	-	0.005(3)	-	-
r_1 (pole)	0.348(6)	0.331(1)	0.352(1)	0.354(1)	0.358(2)	0.262(1)	0.259(0)
r_1 (side)	0.366(6)	0.347(1)	0.371(1)	0.373(1)	0.377(3)	0.273(2)	0.271(1)
r_1 (back)	0.402(8)	0.384(1)	0.407(1)	0.406(1)	0.410(3)	0.308(2)	0.307(1)
r_2 (pole)	0.379(2)	0.398(4)	0.375(2)	0.364(3)	0.362(8)	0.462(3)	0.468(3)
r_2 (side)	0.400(2)	0.422(5)	0.396(2)	0.382(3)	0.381(10)	0.497(4)	0.506(4)
r_2 (back)	0.434(4)	0.455(7)	0.430(3)	0.414(5)	0.413(15)	0.523(5)	0.533(6)
f	11(2)%	14(4)%	13(2)%	5(3)%	2(8)%	7(7)%	11(7)%
Spot	Star 1	Star 2	Star 1	-	-	Star 1	Star 2
Colatitude (deg)	52(2)	26(1)	52	-	-	47(4)	45(2)
Longitude (deg)	134(1)	98(4)	134	-	-	239(1)	244(2)
Diameter (deg)	22(0)	25(0)	22	-	-	17(0)	14(0)
T-factor	1.14(00)	0.83(00)	1.14	-	-	1.29(1)	0.72(1)
$\Sigma W(O-C)^2$	7.18×10^{-8}	9.44×10^{-8}	6.46×10^{-8}	7.26×10^{-8}	7.23×10^{-8}	1.20×10^{-7}	1.00×10^{-7}

4 STUDY OF ORBITAL PERIOD

There has been no analysis of orbital period since these three targets were discovered. Therefore, we analyzed all light minima that we could obtain. There are a total of 11 for FP Lyn, 34 for FV CVn and 13 for V354 UMa. All of these minima are listed in the first columns of Tables 4, 5 and 6, respectively. The linear ephemerides that are applied

Table 4 Observed Times and $O-C$ Values of Minimum Light for FP Lyn

JD(Hel.) 2400000+	Error	Type	Min.	Epoch	$(O-C)$	Residual	Reference
53045.9320		ccd or pe	p	0	0.0000	0.0000	[1]
57101.4357	0.0041	pe	p	11294	–0.0023	–0.0006	[2]
57101.6149	0.0020	pe	s	11294.5	–0.0026	–0.0010	[2]
57122.4435	0.0004	ccd	s	11352.5	–0.0010	0.0006	[3]
57329.6355	0.0007	ccd	s	11929.5	–0.0010	–0.0008	[3]
57465.3743	0.0005	ccd	s	12307.5	0.0037	0.0029	[3]
57790.1618		ccd	p	13212	–0.0012	–0.0045	[4]
57790.3491		ccd	s	13212.5	0.0065	0.0032	[4]
57418.6891	0.0037	ccd	s	12177.5	–0.0005	–0.0009	[5]
57418.8717	0.0014	ccd	p	12178	0.0026	0.0022	[5]
57438.7979	0.0016	ccd	s	12233.5	–0.0004	–0.0010	[5]

Notes: [1] GCVS; [2] Hubscher (2016); [3] Juryšek et al. (2017); [4] VSOLJ 64; [5] This paper.

Table 5 Observed Times and $O-C$ Values of Minimum Light for FV CVn

JD(Hel.) 2400000+ (1)	Error (2)	Method (3)	Min. (4)	Epoch (5)	$(O-C)_1$ (6)	$(O-C)_2$ (7)	Residual (8)	Reference (9)
51251.8239	0.0007	ccd	s	–5687.5	–0.0137	0.0031	–0.0031	[1]
51259.8720	0.0005	ccd	p	–5662	–0.0074	0.0093	0.0030	[1]
53045.4760	0.0009	ccd	p	0	0.0000	–0.0068	–0.0018	[2]
53060.4579	0.0013	ccd	s	47.5	0.0021	–0.0049	0.0002	[2]
53060.6181	0.0020	ccd	p	48	0.0046	–0.0024	0.0027	[2]
53068.4984	0.0018	ccd	p	73	0.0008	–0.0063	–0.0012	[2]
53081.4294	0.0019	ccd	p	114	0.0018	–0.0053	–0.0002	[2]
53094.3569	0.0012	ccd	p	155	–0.0007	–0.0079	–0.0027	[2]
53094.5212	0.0021	ccd	s	155.5	0.0059	–0.0013	0.0039	[2]
53117.3811	0.0017	ccd	p	228	0.0019	–0.0056	–0.0002	[2]
53117.5393	0.0011	ccd	s	228.5	0.0024	–0.0050	0.0003	[2]
53464.4430	0.0020	ccd	s	1328.5	0.0046	–0.0054	0.0009	[3]
53809.4517	0.0010	pe	s	2422.5	0.0040	–0.0081	–0.0025	[4]
53936.3887	0.0008	pe	p	2825	0.0066	–0.0061	–0.0015	[5]
54170.3973	0.0002	pe	p	3567	0.0143	0.0008	0.0023	[5]
54544.7391	0.0002	ccd	p	4754	0.0179	0.0035	–0.0009	[6]
54682.3999	0.0011	ccd	s	5190.5	0.0219	0.0074	0.0017	[7]
54913.7168	0.0004	ccd	p	5924	0.0185	0.0040	–0.0023	[8]
55000.4444	0.0003	ccd	p	6199	0.0208	0.0063	0.0001	[9]
55317.3859	0.0001	ccd	p	7204	0.0204	0.0065	0.0014	[10]
55317.5440	0.0001	ccd	s	7204.5	0.0209	0.0069	0.0019	[10]
55629.9079	0.0003	ccd	p	8195	0.0157	0.0028	–0.0003	[11]
56001.8793	0.0006	ccd	s	9374.5	0.0141	0.0030	0.0027	[12]
56010.8612	0.0004	ccd	p	9403	0.0081	–0.0029	–0.0032	[13]
56031.3619	0.0004	pe	p	9468	0.0101	–0.0008	–0.0010	[14]
56034.3584	0.0004	pe	s	9477.5	0.0106	–0.0003	–0.0004	[14]
56069.5211	0.0036	pe	p	9589	0.0101	–0.0006	–0.0004	[14]
56074.7247	0.0003	ccd	s	9605.5	0.0102	–0.0005	–0.0003	[12]
57003.6183	0.0005	ccd	p	12551	–0.0038	–0.0066	–0.0007	[15]
57119.8307	0.0002	ccd	s	12919.5	–0.0034	–0.0049	0.0013	[16]
57433.9306	0.0003	ccd	s	13915.5	–0.0071	–0.0047	0.0014	[17]
57842.9550	0.0002	ccd	s	15212.5	–0.0110	–0.0030	–0.0003	[18]
58229.7505	0.0003	ccd	p	16439	–0.0107	0.0034	–0.0002	[18]
58229.9080	0.0003	ccd	s	16439.5	–0.0109	0.0032	–0.0004	[18]

Notes: [1] Blattler & Diethelm (2004); [2] Diethelm (2004); [3] Diethelm (2005); [4] Diethelm (2006); [5] Diethelm (2007); [6] Nelson (2009); [7] Diethelm (2009a); [8] Nelson (2010); [9] Diethelm (2009b); [10] Demircan et al. (2011); [11] Nelson (2012); [12] Diethelm (2012); [13] Nelson (2013); [14] Hubscher et al. (2013); [15] Juryšek et al. (2017); [16] Nelson (2016); [17] Nelson (2017); [18] This paper.

Table 6 Observed Times and $O - C$ Values of Minimum Light for V354 UMa

JD(Hel.) 2400000+ (1)	Error (2)	Type (3)	Min. (4)	Epoch (5)	$(O - C)$ (6)	Residual (7)	Reference (8)
56008.5255	0.0015	pe	p	0	0.0000	–0.0019	[1]
56016.3144	0.0012	ccd	s	26.5	0.0025	0.0006	[2]
56016.4583	0.0008	ccd	p	27	–0.0005	–0.0024	[2]
56019.4003	0.0024	pe	p	37	0.0033	0.0014	[1]
56019.5476	0.0018	pe	s	37.5	0.0037	0.0018	[1]
57022.9616	0.0005	ccd	s	3452.5	0.0053	–0.0006	[3]
57023.1105	0.0010	ccd	p	3453	0.0072	0.0013	[3]
57097.4494	0.0049	pe	p	3706	0.0084	0.0019	[4]
57100.3855	0.0026	pe	p	3716	0.0063	–0.0002	[4]
57100.5326	0.0031	pe	s	3716.5	0.0065	–0.0001	[4]
57843.7671	0.0007	ccd	p	6246	0.0107	–0.0039	[5]
58231.7783	0.0004	ccd	s	7566.5	0.0259	0.0055	[5]
58231.9164	0.0006	ccd	p	7567	0.0171	–0.0033	[5]

Notes: [1] Hubscher et al. (2013); [2] Gursoytrak et al. (2013); [3] Nelson (2015); [4] Hubscher (2016); [5] This paper.

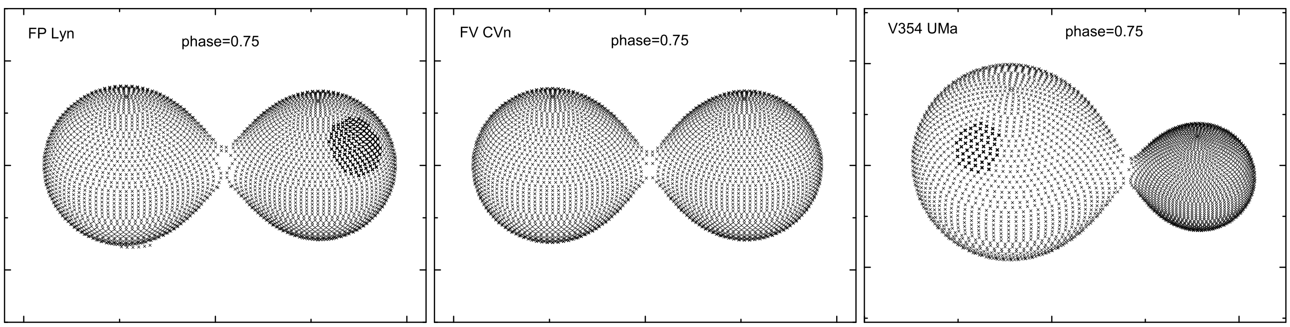

Fig. 5 Geometrical configuration of FP Lyn (*left panel*), FV CVn (*middle panel*) and V354 UMa (*right panel*) at phase 0.75.

to calculate the values of $O - C$ are:

$$\text{FP Lyn: Min.}I = 2453045.932 + 0.35909 \times E, \quad (2)$$

$$\text{FV CVn: Min.}I = 2453045.476 + 0.31537 \times E, \quad (3)$$

$$\text{V354 UMa: Min.}I = 2456008.526 + 0.293825 \times E, \quad (4)$$

where the initial epoch and period are taken from the $O-C$ Gateway. Tables 4, 5 and 6 display the calculated $O - C$ values for these three systems. The data corresponding to $O - C$ values of FP Lyn and V354 UMa are plotted in Figure 6, and the data corresponding to $(O - C)_1$ values of FV CVn are plotted in Figure 7.

As Figure 6 shows, the overall trend of FP Lyn and V354 UMa exhibits nonlinear variations. We used upward pointing parabolas to fit the $O-C$ values. The least squares method was utilized to revise ephemerides for FP Lyn and V354 UMa:

$$\begin{aligned}\text{FP Lyn: Min.}I =& 2453045.9319850(\pm 0.2580064)\\ &+ 0.359082527(\pm 0.000000018) \times E\\ &+ 2.061(\pm 0.014) \times 10^{-10} \times E^2,\\ \text{V354 UMa: Min.}I =& 2456008.5273908(\pm 0.4878153)\\ &+ 0.2938251(\pm 0.000000048) \times E\\ &+ 3.098(\pm 0.065) \times 10^{-10} \times E^2.\end{aligned} \quad (5)$$

In Equation (5), the coefficients of the second-order term are positive, indicating that the periods of FP Lyn and V354 UMa are all secular increases and the rates are calculated as $dp/dt = 4.19(\pm 0.03) \times 10^{-7}\,\mathrm{d\,yr^{-1}}$ and $dp/dt = 7.70(\pm 0.16) \times 10^{-7}\,\mathrm{d\,yr^{-1}}$, respectively. When we removed the parabolic values from the $O - C$ trend, the residuals are plotted in the bottom panels of Figure 6. We can see that the residuals are almost flat, implying the $O - C$ values of FP Lyn and V354 UMa were fitted well with the parabolic terms.

As Figure 7 demonstrates, the data corresponding to the $(O - C)_1$ of FV CVn display a downward parabolic

Table 7 Parameters for the Fit of Times of Minimum Light for FV CVn

Parameter	Value	Error
ΔT_0 (d)	0.00682	$\pm$0.00064
ΔP_0 (d)	2.75×10^{-6}	$\pm 0.16 \times 10^{-6}$
β (d yr^{-1})	-1.13×10^{-6}	$\pm 0.06 \times 10^{-6}$
A_3 (d)	0.0069	$\pm$0.0008
e	0.41	$\pm$0.16
P_3 (yr)	10.28	$\pm$0.42
$\omega(^\circ)$	9.2	$\pm$24.5
T_P (HJD)	2422843.1	$\pm$100244.6

component accompanied by a cyclic variation. Therefore, we used the following equation which is taken from Irwin (1952) to fit the overall trend,

$$\begin{aligned}(O-C)_1 =& T_0 + \Delta T_0 + (P_0 + \Delta P_0)E + \frac{\beta}{2}E^2 \\ &+ A[(1-e^2)\frac{\sin(\nu+\omega)}{(1+e\cos\nu)} + e\sin\omega] \\ =& T_0 + \Delta T_0 + (P_0 + \Delta P_0)E + \frac{\beta}{2}E^2 \\ &+ A[\sqrt{(1-e^2)}\sin E^* \cos\omega + \cos E^* \sin\omega],\end{aligned} \quad (6)$$

where ΔT_0 and ΔP_0 are included to revise the initial ephemeris and period, respectively. β is the value of long-term change in period, A and e are the amplitude and eccentricity of light effect respectively, and ω represents the longitude of periastron. Then, all of the parameters in this equation were determined as listed in Table 7. The value of β is negative which indicates that the variation of the period has a secularly decreasing component with a rate of $dp/dt = -1.13(\pm 0.06) \times 10^{-6}\,\mathrm{d\,yr^{-1}}$. If the long-term decrease is removed, the data of $(O-C)_2$ are plotted in the middle panel of Figure 7 and periodic oscillation is seen clearly. The final fitting result shows that the amplitude and period of this oscillation are 0.0069 d and 10.28 yr, respectively. The residuals are displayed in the bottom panel of Figure 7 when the cyclic oscillation is removed. All these residuals seem to be near zero which indicates that almost no change can be found. Therefore, the data of $(O-C)_1$ were fitted well by using Equation (6).

5 SUMMARY AND CONCLUSIONS

Photometric solutions were determined by the multi-band light curves by using the W-D program. Through analysis of the final fitting parameters, we can obtain the following conclusions. All of these three systems, FP Lyn, FV CVn and V354 UMa, are shallow contact binaries with fill-out factors of $f = 13.4 \pm 1.9\%$, $f = 4.6 \pm 2.5\%$ and $f = 10.7 \pm 6.8\%$, respectively. Because the mass ratios of these three systems are all greater than 1, they are all W-subtype binary systems. The mass ratios of FP Lyn, FV CVn and V354 UMa are $q = 1.153 \pm 0.006$, $q = 1.075 \pm 0.010$ and $q = 3.623 \pm 0.040$, respectively. As the spectra or the radial velocity curves of these three targets are all absent, the absolute parameters cannot be determined directly. The absolute parameters were determined by using the three-dimensional correlations of physical parameters for contact binaries taken from Gazeas (2009). The separations between two components were calculated using Kepler's third law. All of the absolute parameters for these three systems are listed in Table 8.

5.1 Mass Transfer and Possible Evolution

From the analysis of orbital period for FP Lyn and V354 UMa, the overall trend of $O - C$ shows upward parabolic compositions with a rate of $dp/dt = 4.19(\pm 0.03) \times 10^{-7}\,\mathrm{d\,yr^{-1}}$ and $dp/dt = 7.70(\pm 0.16) \times 10^{-7}\,\mathrm{d\,yr^{-1}}$, respectively. The long-term increase can probably be explained by mass transfer from the less massive star to the more massive star. Then, the following equation was used to calculate the rate of mass transfer for FP Lyn and V354 UMa,

$$\frac{\dot{P}}{P} = -3\dot{M}_1\left(\frac{1}{M_1} - \frac{1}{M_2}\right) \ . \quad (7)$$

Combining the parameters including mass, period and rate of period variation, the rate of mass transfer was determined as $dM_1/dt = -2.83 \times 10^{-6}\,M_\odot\,\mathrm{yr}^{-1}$ and $dM_1/dt = -3.50 \times 10^{-7}\,M_\odot\,\mathrm{yr}^{-1}$ respectively. The negative sign indicates that the less massive component M_1 is losing mass, while the more massive component M_2 is receiving mass. As the mass ratio increases, so does the separation between the two components. The degree of contact will decrease. They will evolve from the present configuration of contact binaries to semi-contact or detached binaries. This is not the end of evolution. According to the theory of stellar evolution, the more massive component will fill its Roche lobe first, and the mass would be transferred from the more massive star to the less massive one. Therefore, these two systems are good targets for studying the TRO model (e.g., Lucy 1976; Flannery 1976; Robertson & Eggleton 1977), and we need to observe them continually.

The secular period decrease can be generally explained by mass transfer and AML by stellar wind. Firstly, assuming the long-term decrease of FV CVn is owing to mass transfer from the more massive component to the less massive component, the rate of mass transfer

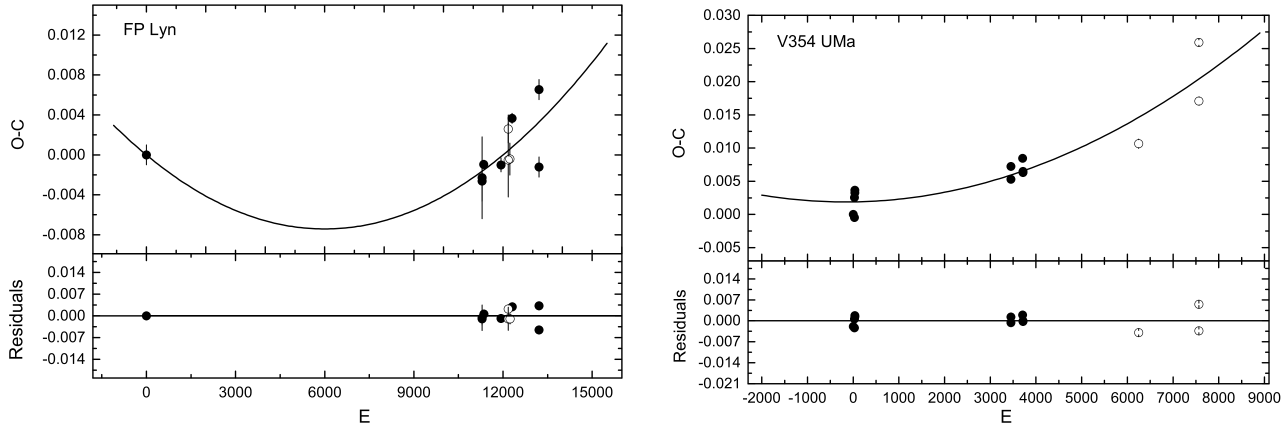

Fig. 6 $O-C$ diagram of FP Lyn (*left panel*) and V354 UMa (*right panel*). The upper panels display the $O-C$ curve determined by the linear ephemeris of Eq. (2) based on all available times of minimum light. The residual values which remove the quadratic term from the $O-C$ curve are plotted in the lower panels. *Open circles* refer to the light minima from our observations, while *filled circles* represent the data from other literature.

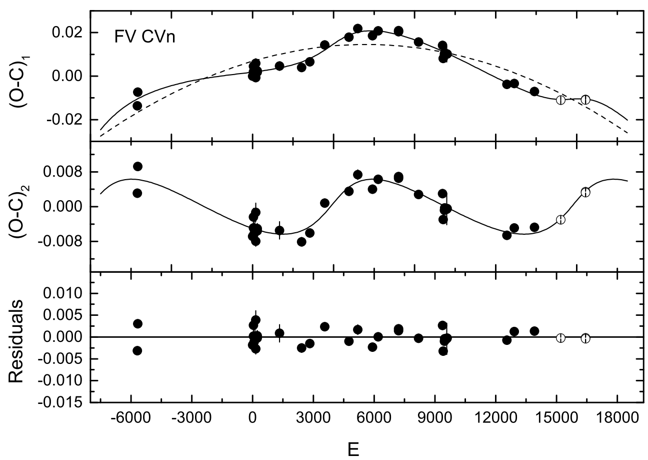

Fig. 7 $O-C$ diagram of FV CVn. The *top panel* shows the $(O-C)_1$ curve determined by the linear ephemeris of Equation (3) based on all available times of minimum light. The $(O-C)_2$ values which remove the quadratic term from the $(O-C)_1$ curve are plotted in the *middle panel*. The residuals from full ephemeris of Eq. (7) are displayed in the *bottom panel*. *Open circles* refer to the light minima from our observations, while *filled circles* represent the data from other literature.

Table 8 Absolute Parameters of FP Lyn, FV CVn and V354 UMa

Object	FP Lyn		FV CVn		V354 UMa	
Parameter	Value	Error	Value	Error	Value	Error
M_1 ($M_\odot$)	0.97	0.09	0.94	0.09	0.29	0.05
M_2 ($M_\odot$)	1.11	0.11	1.01	0.10	1.05	0.12
R_1 ($R_\odot$)	1.01	0.05	0.91	0.05	0.60	0.04
R_2 ($R_\odot$)	1.07	0.05	0.94	0.04	1.04	0.06
L_1 ($L_\odot$)	0.90	0.10	0.66	0.08	0.36	0.05
L_2 ($L_\odot$)	1.02	0.12	0.71	0.09	1.10	0.18
a ($R_\odot$)	2.72	0.14	2.44	0.13	2.05	0.14

was determined as $dM_1/dt = 1.61 \times 10^{-5}\,M_\odot\,\mathrm{yr}^{-1}$ by using Equation (7). The positive sign indicates that the less massive component M_1 is receiving mass from M_2. Considering the mass of the secondary star, the timescale of mass transfer was calculated as $\tau \sim \frac{M_2}{\dot{M}_2} \sim 6.28 \times 10^4$ yr, which is about $\frac{1}{764}$ times the thermal timescale of the secondary star ($\frac{GM^2}{RL} \sim 4.79 \times 10^7$ yr). Hence, mass transfer cannot be used to explain the long-term change in composition of FV CVn. The evolution of FV CVn is mainly driven by AML via magnetic braking. We compiled information on other shallow contact W-subtype eclipsing binaries, and their periods manifest secular decrease. As shown in Table 9, the rate of long-term decrease for FV CVn is the biggest among these objects, so we cannot exclude the possibility that it is undergoing a long-term periodic change.

5.2 Are FP Lyn, FV CVn and V354 UMa All Triple Systems?

As depicted in Figure 7, after the downward quadratic term in the $(O-C)_1$ curves is removed, the $(O-C)_2$ data indicate it is a periodic oscillation. The amplitude and period of this sinusoidal variation are 0.0069 d and 10.28 yr respectively. Cyclic variations are generally caused by the Applegate mechanism (Applegate 1992) or the light travel time effect (LTTE) by a third body.

The Applegate mechanism (Applegate 1992) occurs when magnetic activity makes the quadrupole moment change, giving rise to variation of the orbital period. Assuming the magnetic cycle in the quadrupole moment of the primary component causes the periodic oscillation, the following equation, which was taken from Lanza & Rodono (2002), was used to calculate the quadrupole moment,

$$\frac{\Delta P}{P} = -9\frac{\Delta Q}{Ma^2} \ . \tag{8}$$

The required variation of the quadruple moment for the primary star $\Delta Q = 9.1 \times 10^{49}\,\mathrm{g\,cm^2}$ was determined using this equation, which is about two orders of magnitude smaller than the typical value of 10^{51} to $10^{52}\,\mathrm{g\,cm^2}$. Therefore, the Applegate mechanism cannot explain the periodic variation.

The most likely reason leading to the cyclic variations in the $(O-C)_2$ curve of FV CVn is the LTTE via the existence of a third body (e.g., Liao & Qian 2010). There are many other examples to support this view, such as BI Vul (Qian et al. 2013b), TY UMa (Li et al. 2015c), V776 Cas (Zhou et al. 2016c) and UZ Leonis (Lee & Park 2018). Therefore, the following equation was applied to calculate the parameters of the third body,

$$f(m) = \frac{(m_3 \sin i^{'})^3}{(m_1+m_2+m_3)^2} = \frac{4\pi}{GP_3^2} \times (a_{12} \sin i^{'})^3. \tag{9}$$

$f_3(m) = 1.62(\pm 0.56) \times 10^{-2}\,M_\odot$ for the additional component was determined. It was assumed that the orbital inclination of the third body $i^{'}$ and the orbital plane of the eclipsing binary FV CVn are coplanar ($i^{'} = i = 64.2°$). Then the mass of the third body was obtained as $m_3 = 0.411(\pm 0.086)\,M_\odot$ with a distance of $5.05(\pm 1.20)$ AU. Therefore, assuming the third body is a main sequence star, then the luminosity was calculated as $L_3 = 0.04\,L_\odot$ according to Cox (2000), which accounts for about 2.5% of the triple system of FV CVn. According to the previous photometric solutions, the ratio of the third light is too small, just about 0.5%. Although this also demonstrates that a third light may exist, we still choose the result without the third light in the final fitting result. However, FV CVn could still be a triple system.

Through analysis of the evolution and presence of a third body associated with FV CVn, a comprehensive analysis of its evolution process was obtained. According to the statistical analysis of Stepien & Gazeas (2012), low mass contact binaries (LMCBs) whose total mass is lower than $1.4\,M_\odot$ would be in pre-contact phase for a long time of 8-9 Gyr, nevertheless, the contact phase lasts for about only 0.8 Gyr. In addition, such systems show very short periods ($P < 0.3$ d) along with moderate mass ratios ($0.2 \leq q \leq 0.8$). Thus the progenitor of FV CVn may be a short-period detached system with two main sequence stars, and the case of FV CVn is highly similar to that of BI Vul (Qian et al. 2013b). The fill-out factor $f = 4.6\%$ further supports the assumption that it is a newly formed shallow contact binary and is in the initial state of contact. From the orbital period analysis, no mass transfer occurred between two components because the timescale of mass transfer is very short. Therefore, it evolved into the presently shallow contact configuration due to the AML via magnetic braking. Admittedly, a third body played an important role in the evolution of FV CVn. Angular momentum may be lost from the central pair to the additional component via the Kozai mechanism (Kozai 1962), and in addition AML will cause the orbital period to decrease and lead to the contact degree increasing. Eventually, it will evolve into a deep contact phase (e.g., M4 V53, Li et al. 2017; NO Cam, Zhou et al. 2017) or merge into a rapidly rotating single star (e.g., Stepien & Gazeas 2012; Qian et al. 2013b).

Although the orbital period analysis of FP Lyn and V354 UMa did not find any component of periodic change, the third light component was identified in the photometric analysis of FP Lyn, and its proportion cannot be ignored. This suggests that FP Lyn could be a triple system. Meanwhile, we cannot rule out the possibility that V354 UMa is a triple system, maybe the third body of V354 UMa is too dim to record.

In summary, FP Lyn, FV CVn and V354 UMa are all W-subtype W UMa stars. The light curves of FP Lyn and V354 UMa are asymmetric, therefore, spots were added in the process of calculating parameters. The overall trends of

Table 9 W-subtype Shallow Contact Binaries with Decreasing Orbital Period

Star	Period (d)	q	$f(\%)$	T_1 (K)	T_2 (K)	dp/dt (d yr^{-1})	Reference
MR Com	0.412746	3.912	10.0%	6530	6442	-5.3×10^{-7}	Qian et al. (2013a)
V1007 Cas	0.332008	3.363	8.1%	5135	4193	-1.8×10^{-7}	Li et al. (2018)
SS Ari	0.405991	3.250	9.4%	5950	5745	-4.0×10^{-7}	Liu et al. (2009)
BX Peg	0.280422	2.660	14.6%	5887	5300	-2.1×10^{-7}	Li et al. (2015a); Lee et al. (2009)
V396 Mon	0.396344	2.554	18.9%	6210	6121	-8.6×10^{-8}	Liu et al. (2011a)
LO Com	0.286361	2.478	3.2%	5178	4875	-1.2×10^{-7}	Zhang et al. (2016)
VW Boo	0.342318	2.336	10.8%	5560	5198	-1.5×10^{-7}	Liu et al. (2011b)
GU Ori	0.470682	2.320	17.7%	6050	6021	-6.2×10^{-8}	Zhou et al. (2018)
TY Boo	0.317150	2.150	16.4%	5712	5108	-3.7×10^{-8}	Christopoulou et al. (2012)
BM UMa	0.271220	1.852	17.0%	4982	4600	-9.8×10^{-8}	Samec et al. (1995)
V1139 Cas	0.297101	1.583	3.6%	6250	5933	-3.7×10^{-7}	Li et al. (2015b)
IK Boo	0.303117	1.146	2.2%	5781	5422	-2.2×10^{-7}	Kriwattanawong et al. (2017)
FV CVn	0.315365	1.075	4.6%	5470	5120	-1.1×10^{-6}	This paper

$O-C$ for FP Lyn and V354 UMa are all upward parabolic curves, revealing that the periods of both of them are undergoing prolonged increase. This may be explained by mass transfer from the less massive star to the more massive star. While the $(O-C)_1$ curve of FV CVn manifests a downward variation, after verification the long-term decrease cannot be explained by mass transfer, and AML due to magnetic activity may cause this phenomenon. The periodic oscillation of FV CVn is most likely to be due to a third body through the analysis of orbital period and photometric solutions with added third light. In addition, a third light was also added in the photometric solutions of FP Lyn and V354 UMa, and finally we procured a convergent solution for FP Lyn, but a convergent solution for V354 UMa was not generated. This suggests that FP Lyn could be a triple system, therefore more light minima of these three systems are needed to obtain the $O-C$ curves to analyze the period variation. Although the results we obtained are very reliable, the radial velocity curves can further confirm the obtained mass ratios and absolute parameters. Therefore, more observations combining photometry and spectra are needed for these three systems.

Acknowledgements RM acknowledges financial support from the Universidad Nacional Autónoma de México (UNAM) and DGAPA (PAPIIT IN 100918). This work is also supported by the National Natural Science Foundation of China (NSFC) (No. 11703016), and by the Joint Research Fund in Astronomy (No. U1431105) under cooperative agreement between the NSFC and the Chinese Academy of Sciences (CAS), by the Natural Science Foundation of Shandong Province (No. ZR2014AQ019), by the Young Scholars Program of Shandong University, Weihai (No. 20820171006), and by the Open Research Program of Key Laboratory for the Structure and Evolution of Celestial Objects (No. OP201704). The spectral data were provided by the Guo Shou Jing Telescope (the Large Sky Area Multi-Object Fiber Spectroscopic Telescope, LAMOST), which is a National Major Scientific Project built by CAS. Funding for the project has been provided by the National Development and Reform Commission. LAMOST is operated and managed by National Astronomical Observatories, CAS.

References

Akerlof, C., Amrose, S., Balsano, R., et al. 2000, AJ, 119, 1901
Applegate, J. H. 1992, ApJ, 385, 621
Blattler, E., & Diethelm, R. 2004, Information Bulletin on Variable Stars, 5541, 1
Christopoulou, P.-E., Papageorgiou, A., Vasileiadis, T., & Tsantilas, S. 2012, AJ, 144, 149
Cox, A. N. 2000, Introduction, ed. A. N. Cox, Allen's Astrophysical Quantities, ed. A. N. Cox (New York: AIP Press; Springer), 1
Demircan, Y., Gurol, B., Gokay, G., et al. 2011, Information Bulletin on Variable Stars, 5965, 1
Diethelm, R. 2004, Information Bulletin on Variable Stars, 5543
Diethelm, R. 2005, Information Bulletin on Variable Stars, 5653
Diethelm, R. 2006, Information Bulletin on Variable Stars, 5713
Diethelm, R. 2007, Information Bulletin on Variable Stars, 5781
Diethelm, R. 2009a, Information Bulletin on Variable Stars, 5871
Diethelm, R. 2009b, Information Bulletin on Variable Stars, 5894
Diethelm, R. 2012, Information Bulletin on Variable Stars, 6029
Flannery, B. P. 1976, ApJ, 205, 217
Gazeas, K. D. 2009, Communications in Asteroseismology, 159, 129
Guo, D. F., Li, K., Hu, S. M., & Chen, X. 2018, PASP, 130, 064201
Gursoytrak, H., Demircan, Y., Gokay, G., et al. 2013, Information Bulletin on Variable Stars, 6075
Hoffman, D. I., Harrison, T. E., & McNamara, B. J. 2009, AJ, 138, 466

Hubscher, J. 2016, Information Bulletin on Variable Stars, 6157
Hubscher, J., Braune, W., & Lehmann, P. B. 2013, Information Bulletin on Variable Stars, 6048
Irwin, J. B. 1952, ApJ, 116, 211
Juryšek, J., Hoňková, K., Šmelcer, L., et al. 2017, Open European Journal on Variable Stars, 179, 1
Khruslov, A. V. 2006, Peremennye Zvezdy Prilozhenie, 6, 30
Kriwattanawong, W., Sanguansak, N., & Maungkorn, S. 2017, PASJ, 69, 62
Kozai, Y. 1962, AJ, 67, 446
Lanza, A. F., & Rodonò, M. 2002, Astron. Nachr., 323, 424
Lee, J. W., & Park, J.-H. 2018, PASP, 130, 034201
Lee, J. W., Kim, S.-L., Lee, C.-U., et al. 2009, PASP, 121, 1366
Li, K., Qian, S.-B., Hu, S.-M., & He, J.-J. 2014, AJ, 147, 98
Li, K., Hu, S., Guo, D., et al. 2015a, New Astron., 41, 17
Li, K., Hu, S.-M., Guo, D.-F., et al. 2015b, New Astron., 34, 217
Li, K., Hu, S.-M., Guo, D.-F., et al. 2015c, AJ, 149, 120
Li, K., Gao, D.-Y., Hu, S.-M., et al. 2016a, Ap&SS, 361, 63
Li, K., Hu, S.-M., Guo, D.-F., et al. 2016b, Journal of Astrophysics and Astronomy, 37, 16
Li, K., Hu, S., Chen, X., & Guo, D. 2017, PASJ, 69, 79
Li, K., Xia, Q.-Q., Hu, S.-M., Guo, D.-F., & Chen, X. 2018, PASP, 130, 074201
Liao, W.-P., & Qian, S.-B. 2010, MNRAS, 405, 1930
Liao, W.-P., Qian, S.-B., & Liu, N.-P. 2012, AJ, 144, 178
Liao, W.-P., Qian, S.-B., Soonthornthum, B., et al. 2017, PASP, 129, 124204
Liu, L., Qian, S.-B., He, J.-J., Zhang, J., & Li, L.-J. 2009, Ap&SS, 321, 19
Liu, L., Qian, S.-B., Liao, W.-P., et al. 2011a, AJ, 141, 44
Liu, L., Qian, S.-B., Zhu, L.-Y., He, J.-J., & Li, L.-J. 2011b, AJ, 141, 147
Lucy, L. B. 1968a, ApJ, 153, 877
Lucy, L. B. 1968b, ApJ, 151, 1123
Lucy, L. B. 1976, ApJ, 205, 208
Luo, A.-L., Zhao, Y.-H., Zhao, G., et al. 2015, RAA (Research in Astronomy and Astrophysics), 15, 1095
Maciejewski, G., & Niedzielski, A. 2005, Baltic Astronomy, 14, 205
Nelson, R. H. 2009, Information Bulletin on Variable Stars, 5875
Nelson, R. H. 2010, Information Bulletin on Variable Stars, 5929
Nelson, R. H. 2012, Information Bulletin on Variable Stars, 6018
Nelson, R. H. 2013, Information Bulletin on Variable Stars, 6050
Nelson, R. H. 2015, Information Bulletin on Variable Stars, 6131
Nelson, R. H. 2016, Information Bulletin on Variable Stars, 6164
Nelson, R. H. 2017, Information Bulletin on Variable Stars, 6195
Norton, A. J., Wheatley, P. J., West, R. G., et al. 2007, A&A, 467, 785
Qian, S. 2001a, MNRAS, 328, 635
Qian, S. 2001b, MNRAS, 328, 914
Qian, S. 2003, MNRAS, 342, 1260
Qian, S.-B., Yuan, J.-Z., Soonthornthum, B., et al. 2007, ApJ, 671, 811
Qian, S.-B., Liu, N.-P., Liao, W.-P., et al. 2013a, AJ, 146, 38
Qian, S.-B., Liu, N.-P., Li, K., et al. 2013b, ApJS, 209, 13
Qian, S.-B., He, J.-J., Zhang, J., et al. 2017, RAA (Research in Astronomy and Astrophysics), 17, 087
Qian, S.-B., Zhang, J., He, J.-J., et al. 2018, ApJS, 235, 5
Rahunen, T. 1981, A&A, 102, 81
Robertson, J. A., & Eggleton, P. P. 1977, MNRAS, 179, 359
Ruciński, S. M. 1969, Acta Astronomica, 19, 125
Samec, R. G., Gray, J. D., Carrigan, B. J., & Kreidl, T. J. 1995, PASP, 107, 136
Stepien, K., & Gazeas, K. 2012, AcA, 62, 153
van Hamme, W. 1982, A&A, 105, 389
van Hamme, W. 1993, AJ, 106, 2096
vant Veer, F. 1979, A&A, 80, 287
Woźniak, P. R., Vestrand, W. T., Akerlof, C. W., et al. 2004, AJ, 127, 2436
Yuan, J., & Qian, S. 2007, MNRAS, 381, 602
Zhang, Y., Han, Q. W., & Liu, J. Z. 2016, PASP, 128, 124201
Zhou, X., Qian, S.-B., Essam, A., He, J.-J., & Zhang, B. 2016a, New Astron., 47, 3
Zhou, X., Qian, S. B., Huang, B. H., Li, H., & Zhang, J. 2016b, PASJ, 68, 102
Zhou, X., Qian, S.-B., Zhang, J., et al. 2016c, ApJ, 817, 133
Zhou, X., Qian, S., & Zhang, B. 2017, PASJ, 69, 37
Zhou, X., Qian, S., Boonrucksar, S., et al. 2018, PASJ, 70, 87